nature geoscience

Article

https://doi.org/10.1038/s41561-023-01226-y

Carbonate record of temporal change in oxygen fugacity and gaseous species in asteroid Ryugu

Received: 21 December 2022

Accepted: 14 June 2023

Published online: 10 July 2023

Check for updates

A list of authors and their affiliations appears at the end of the paper

The Hayabusa2 spacecraft explored asteroid Ryugu and brought its surface materials to Earth. Ryugu samples resemble Ivuna-type (CI) chondrites—the most chemically primitive meteorites—and contain secondary phyllosilicates and carbonates, which are indicative of aqueous alteration. Understanding the conditions (such as temperature, redox state and fluid composition) during aqueous alteration is crucial to elucidating how Ryugu evolved to its present state, but little is known about the temporal changes in these conditions. Here we show that calcium carbonate (calcite) grains in Ryugu and Ivuna samples have variable $^{18}O/^{16}O$ and $^{13}C/^{12}C$ ratios that are, respectively, 24–46‰ and 65–108‰ greater than terrestrial standard values, whereas those of calcium–magnesium carbonate (dolomite) grains are much more homogeneous, ranging within 31–36‰ for oxygen and 67–75‰ for carbon. We infer that the calcite precipitated first over a wide range of temperatures and oxygen partial pressures, and that the proportion of gaseous CO_2/CO/CH_4 molecules changed temporally. By contrast, the dolomite formed later in a more oxygen-rich and thus CO_2-dominated environment when the system was approaching equilibrium. The characteristic isotopic compositions of secondary carbonates in Ryugu and Ivuna are not observed for other hydrous meteorites, suggesting a unique evolutionary pathway for their parent asteroid(s).

The Japan Aerospace Exploration Agency Hayabusa2 spacecraft explored the near-Earth asteroid 162173 Ryugu and brought samples of its surface materials back to Earth[1,2]. Ryugu has been classified spectroscopically as a member of the C-complex asteroids[3,4]. It is a rubble-pile asteroid consisting of numerous rocky blocks that are the fragments resulting from the disruption of an original, larger parent body[5–7].

Previous work has reported that Ryugu materials underwent extensive aqueous alteration as the result of water activity in the original parent body[8–10] and are composed mainly of secondary minerals that formed during the aqueous alteration: phyllosilicates, carbonates, sulfides and oxides. Primary minerals such as anhydrous silicates are rare[9]. These petrological characteristics are comparable to those in the CI (Ivuna-type) chondritic meteorites, pointing to a kinship between Ryugu and CI chondrites. The Ryugu's whole-rock chemical and isotope compositions confirm a close affinity with CI chondrites[8,11,12].

Carbonates, the major Ca budget in Ryugu and CI chondrites[13], are of particular interest because (1) their chemical and isotopic compositions reflect the conditions of aqueous alteration and (2) their grain size is commonly large enough to allow in-situ analysis by electron and ion microprobes[14–17]. The C source of carbonates is unclear but was probably ices that included CO, CO_2 and CH_4 and/or organic matter[18,19]. These materials may have formed in the solar nebula or even the parental molecular cloud of the Solar System. Therefore, the C isotope compositions recorded by carbonates can help us shed light on the physicochemical processes that operated in these environments.

e-mail: wataru.fujiya.sci@vc.ibaraki.ac.jp

https://doi.org/10.1038/s41561-023-01226-y

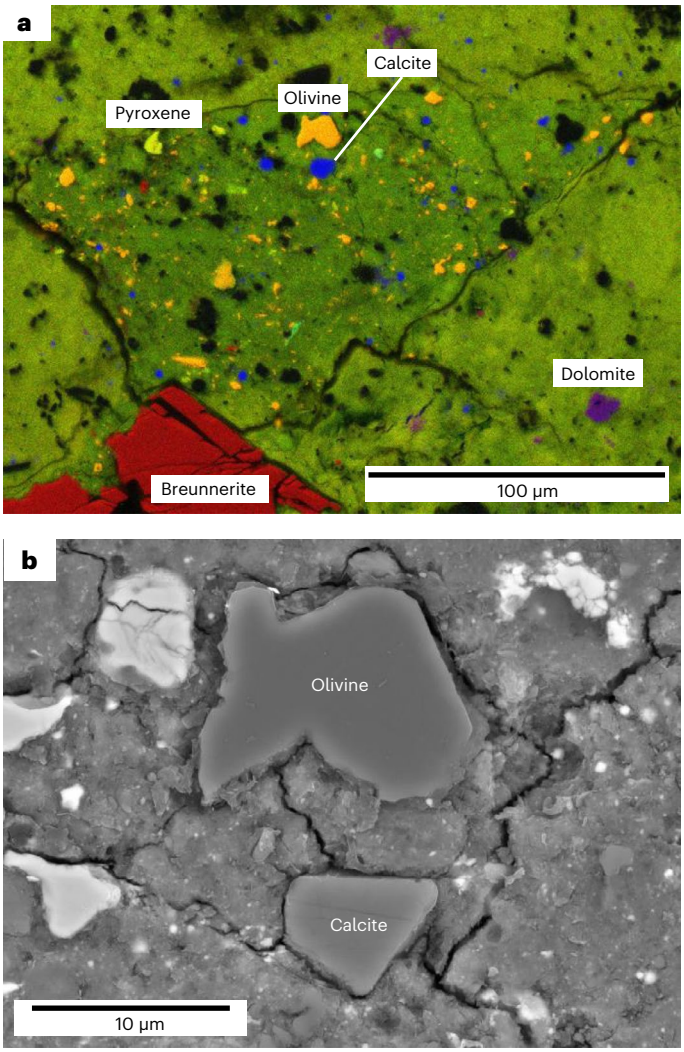

Fig. 1 | Calcite grains in the Ryugu C0002 sample. a, Mg (red), Si (green) and Ca (blue) elemental maps showing the distribution of calcite grains. Calcite grains (blue) in the Ryugu and Ivuna samples can be found in limited areas with Mg-rich olivine (yellow) and pyroxene (light green). Purple grains are dolomite. The large red grain is breunnerite. **b**, Backscattered electron image of a calcite grain.

In this Article, we investigate the conditions of aqueous alteration and the origin of the materials accreted by the Ryugu/CI parent bodies. To this end, we performed in-situ O and C isotope measurements of calcite ($CaCO_3$) and dolomite ($CaMg(CO_3)_2$) in Ryugu samples A0058 (collected at the first touchdown site) and C0002 (from the second touchdown site) as well as the Ivuna meteorite. The O isotope data of the A0058 and Ivuna dolomite are taken from a previous study[8].

Occurrences and isotope compositions of carbonate minerals

Dolomite is the most abundant carbonate mineral in the analysed samples, and we found numerous dolomite grains throughout the Ryugu and Ivuna matrices, whereas calcite is rare. No calcite grains were observed in the Ryugu A0058 sample studied. Calcite was found only in limited areas (clasts) of the Ryugu C0002 and Ivuna samples, occurring with primary anhydrous silicate minerals such as Mg-rich olivine and pyroxene (Fig. 1a). The calcite grains (<10 μm in size) are usually smaller than the dolomite grains (several tens of micrometres) (Fig. 1b). The dolomite has compositional variation and complex zoning within grains (Extended Data Fig. 1). We also found breunnerite ($Mg(Fe,Mn)(CO_3)_2$) grains, for which we did not measure isotope compositions because of the lack of a suitable standard material for isotope analysis.

The O and C isotope compositions of the Ryugu and Ivuna carbonates are similar (Table 1). The $\delta^{18}O$ values of the calcite in C0002 and Ivuna (+24‰ to +46‰) show a grain-to-grain variation larger than those of the dolomite in C0002, A0058 and Ivuna (+26‰ to +31‰) ($\delta^{i}O$ in ‰ = $[(^{i}O/^{16}O)_{sample}/(^{i}O/^{16}O)_{VSMOW} - 1] \times 1{,}000$; i = 17 or 18, and VSMOW is the terrestrial standard material Vienna standard mean ocean water) (Fig. 2a). The simple average of the $\Delta^{17}O$ values, the deviation from the terrestrial fractionation line defined as $\Delta^{17}O = \delta^{17}O - 0.52 \times \delta^{18}O$, of the C0002 and Ivuna calcite is +1.37 ± 0.40‰ (2 s.e., N = 17). The $\Delta^{17}O$ values of the C0002, A0058 and Ivuna dolomite are systematically lower than those of the calcite, and the average $\Delta^{17}O$ value of the dolomite (+0.26 ± 0.23‰, 2 s.e., N = 16) is closer to the whole-rock values of three Ryugu samples[8] (+0.61 ± 0.28‰, 2 s.d.; Fig. 2b). The previously measured O isotope compositions of the A0058 and Ivuna dolomite are in good agreement with those of the C0002 dolomite measured in this study[8].

Like the $\delta^{18}O$ values, the dolomite in A0058, C0002 and Ivuna has a relatively narrow range of $\delta^{13}C$ values, from +67‰ to +75‰ ($\delta^{13}C$ in ‰ = $[(^{13}C/^{12}C)_{sample}/(^{13}C/^{12}C)_{VPDB} - 1] \times 1{,}000$; VPDB is the terrestrial standard material, Vienna PeeDee Belemnite) (Fig. 3). The $\delta^{13}C$ and $\delta^{18}O$ values of the dolomite are broadly consistent with the bulk $\delta^{13}C$ and $\delta^{18}O$ values of carbonates, including calcite, dolomite and breunnerite, in CI chondrites (Ivuna and Orgueil) determined on whole-rock samples[18], corroborating the observation that dolomite is the major carbonate mineral. However, the $\delta^{13}C$ values of the calcite in C0002 and Ivuna are highly heterogeneous from grain to grain, ranging from +65‰ to +108‰, and they are commonly higher than those of the Ryugu and Ivuna dolomite (Fig. 3). These variations have also been reported for other Ryugu samples[20], confirming that our results represent the isotopic characteristics of Ryugu carbonates. For calcite grains on which we conducted multiple measurements, the $\delta^{13}C$ values in each grain are identical within uncertainties of ~5.1‰. Thus, the heterogeneity of $\delta^{13}C$ values within individual calcite grains is probably no larger than 10‰, which is much smaller than the heterogeneity of >40‰ between grains.

Isotope signatures of the Ryugu and CI carbonates

If the carbonates were in O and C isotopic equilibrium with the aqueous fluid when they precipitated, their O and C isotope compositions would have been determined by the mass-dependent equilibrium isotopic fractionation between carbonates and water for O, and that between carbonates and dissolved CO_3^{2-} (and other dissolved C-bearing chemical species) for C. The magnitude of this equilibrium isotopic fractionation depends on temperature[21]. Thus, the O and C isotope compositions of the carbonates would reflect those of water and CO_3^{2-} as well as their formation temperatures. Assuming equilibrium, the temperature of dolomite–magnetite precipitation in the Ryugu A0058 sample analysed previously is estimated to be 37 ± 10 °C (ref. 8), while the inferred alteration temperatures of CI chondrites range up to 150 °C (ref. 22). The equilibrium O isotopic fractionation between water and calcite leads to the enhancement of $\delta^{18}O$ values in calcite relative to water by approximately +38‰, +28‰ and +13‰ at 0, 40 and 150 °C, respectively[23]. Thus, the $\delta^{18}O$ variation of ~22‰ observed in the Ryugu calcite (Fig. 2) is potentially explained by formation temperatures that varied from 0 to 150 °C assuming a fixed $\delta^{18}O$ value of water.

However, this argument does not necessarily mean that variable formation temperature is the sole explanation for the observed $\delta^{18}O$ variation of the calcite. Indeed, the lack of a simple correlation between $\delta^{18}O$ and $\delta^{13}C$ values (Fig. 3) implies that variable formation temperatures alone cannot explain the observed $\delta^{18}O$ and $\delta^{13}C$ variations because the $\delta^{18}O$ and $\delta^{13}C$ values of carbonates should co-vary with their formation temperatures[18]. Rather, it seems likely that the $\delta^{18}O$ value of water and/or the $\delta^{13}C$ value of CO_3^{2-} varied spatially and/or temporally. A previous study used clumped isotope thermometry for carbonates in Mighei-type (CM) chondrites and demonstrated that the $\delta^{18}O$ values of water are variable between samples[16].

https://doi.org/10.1038/s41561-023-01226-y

Table 1 | $\delta^{18}O$, $\delta^{17}O$, $\Delta^{17}O$ and $\delta^{13}C$ values of carbonates in Ryugu and Ivuna samples

Samples	$\delta^{18}O$ (‰)	2σ	$\delta^{17}O$ (‰)	2σ	$\Delta^{17}O$ (‰)	2σ	$\delta^{13}C$ (‰)	2σ
Ryugu C0002, calcite								
Calcite#1a[a]	23.5	0.8	12.5	1.6	0.2	1.5	98.1	4.9
Calcite#1b[a]	23.5	0.8	12.5	1.6	0.2	1.5	92.7	4.8
Calcite#1 average	23.5	0.8	12.5	1.6	0.2	1.5	95.4	3.4
Calcite#2	38.4	0.6	22.2	1.1	2.2	1.1	101.7	4.8
Calcite#3-1	44.3	0.8	24.6	1.4	1.6	1.5	89.9	5.2
Calcite#3-2a[a]	46.3	0.8	25.9	1.6	1.9	1.7	76.2	5.7
Calcite#3-2b[a]	46.3	0.8	25.9	1.6	1.9	1.7	84.5	6.5
Calcite#3-2c[a]	46.3	0.8	25.9	1.6	1.9	1.7	81.0	5.9
Calcite#3-2 average	46.3	0.8	25.9	1.6	1.9	1.7	80.6	3.5
Calcite#3-3	44.5	1.2	24.9	1.5	1.8	1.4	84.1	6.2
Calcite#3-4	42.9	1.2	23.3	1.3	1.0	1.4	87.0	5.6
Calcite#4-1	n.d.		n.d.		n.d.		88.2	5.2
Calcite#4-2	n.d.		n.d.		n.d.		86.1	4.8
Calcite#5a[a]	41.1	1.2	24.2	1.4	2.9	1.4	93.9	4.8
Calcite#5b[a]	40.9	1.2	23.2	1.3	1.9	1.4	93.9	4.8
Calcite#5 average	41.0	0.8	23.7	1.0	2.4	1.0	93.9	4.8
Ivuna, calcite								
Calcite#1	41.6	1.0	22.5	1.3	0.9	1.4	101.5	4.1
Calcite#2	41.5	1.0	23.4	1.3	1.8	1.4	104.8	4.8
Calcite#3	40.7	1.1	21.9	1.6	0.8	1.4	107.1	4.7
Calcite#5	33.9	1.0	20.0	1.3	2.4	1.4	81.4	3.8
Calcite#6	41.1	1.0	24.0	1.4	2.6	1.4	103.9	6.0
Calcite#7	38.0	1.0	20.2	1.4	0.4	1.4	98.0	5.1
Calcite#8-1	37.6	1.0	20.6	1.3	1.1	1.4	79.5	4.4
Calcite#8-2	37.0	1.0	20.0	1.3	0.8	1.4	89.0	5.2
Calcite#9a[a]	36.0	1.0	20.2	1.3	1.5	1.4	106.6	5.8
Calcite#9b[a]	36.0	1.0	20.2	1.3	1.5	1.4	109.9	5.1
Calcite#9c[a]	36.0	1.0	20.2	1.3	1.5	1.4	106.7	4.8
Calcite#9 average	36.0	1.0	20.2	1.3	1.5	1.4	107.8	3.0
Calcite#10a[a]	43.6	0.6	22.3	1.5	−0.4	1.4	65.4	4.7
Calcite#10b[a]	40.9	0.7	21.2	1.2	−0.1	1.2	65.4	4.7
Calcite#10 average	42.2	0.5	21.7	1.0	−0.3	0.9	65.4	4.7
Ryugu A0058, dolomite								
Dolomite#5[a]	(27.0)	(0.9)	(14.2)	(1.0)	(0.2)	(0.9)	67.7	1.5
Dolomite#5[a]	(27.0)	(0.9)	(14.2)	(1.0)	(0.2)	(0.9)	67.2	1.2
Dolomite#5 average	(27.0)	(0.9)	(14.2)	(1.0)	(0.2)	(0.9)	67.5	1.0
Dolomite#2	(29.0)	(1.0)	(15.0)	(1.0)	(0.0)	(0.9)	74.8	1.5
Dolomite#4	(30.0)	(0.9)	(15.8)	(1.0)	(0.2)	(0.9)	72.1	1.3
Dolomite#1	(29.9)	(0.9)	(14.8)	(1.0)	(−0.7)	(0.9)	71.3	1.2
Dolomite#3	(29.5)	(0.8)	(15.7)	(1.0)	(0.4)	(0.9)	74.5	1.5
Ryugu C0002, dolomite								
Dolomite#3a[a]	27.3	1.0	15.2	1.3	1.0	0.9	72.1	1.3
Dolomite#3b[a]	28.1	1.0	14.7	1.3	0.1	0.9	72.1	1.3
Dolomite#3 average	27.7	0.7	14.9	0.9	0.6	0.6	72.1	1.3
Dolomite#4	28.3	1.0	15.3	1.3	0.6	0.9	70.1	1.3
Dolomite#1a[a]	28.6	1.0	15.6	1.3	0.7	0.9	68.1	1.3
Dolomite#1b[a]	28.7	1.0	15.1	1.3	0.2	0.9	68.1	1.3

https://doi.org/10.1038/s41561-023-01226-y

Table 1 (continued) | $\delta^{18}O$, $\delta^{17}O$, $\Delta^{17}O$ and $\delta^{13}C$ values of carbonates in Ryugu and Ivuna samples

Samples	$\delta^{18}O$ (‰)	2σ	$\delta^{17}O$ (‰)	2σ	$\Delta^{17}O$ (‰)	2σ	$\delta^{13}C$ (‰)	2σ
Dolomite#1 average	28.7	0.7	15.4	0.9	0.5	0.6	68.1	1.3
Dolomite#2a[a]	26.7	1.0	14.1	1.3	0.2	0.9	69.4	1.3
Dolomite#2b[a]	27.7	1.0	14.1	1.3	−0.3	0.9	69.5	1.3
Dolomite#2 average	27.2	0.7	14.1	0.9	0.0	0.6	69.4	0.9
Ivuna, dolomite								
Dolomite#1	(29.0)	(0.7)	(15.6)	(0.8)	(0.5)	(0.9)	68.1	1.3
Dolomite#7	(30.8)	(0.7)	(16.0)	(0.8)	(0.0)	(0.7)	68.6	1.1
Dolomite#6	(29.1)	(0.8)	(15.3)	(0.8)	(0.2)	(0.9)	72.3	1.2
Dolomite#5	(28.8)	(0.8)	(16.3)	(0.8)	(1.3)	(0.9)	67.2	1.2
Dolomite#4	(26.5)	(0.9)	(14.4)	(0.9)	(0.7)	(1.0)	68.3	1.3
Dolomite#2a[a]	(29.6)	(0.9)	(15.1)	(0.9)	(−0.3)	(0.8)	67.4	1.3
Dolomite#2b[a]	(29.6)	(0.9)	(15.1)	(0.9)	(−0.3)	(0.8)	65.6	1.3
Dolomite#2c[a]	(29.6)	(0.9)	(15.1)	(0.9)	(−0.3)	(0.8)	67.4	1.3
Dolomite#2 average	(29.6)	(0.9)	(15.1)	(0.9)	(−0.3)	(0.8)	66.8	0.7
Dolomite#3	(29.2)	(1.0)	(15.4)	(1.0)	(0.2)	(1.1)	68.8	1.2

The O isotope compositions of the Ryugu A0058 and Ivuna dolomite, shown in parentheses, are taken from Yokoyama et al.[8]. The 2σ errors are either external reproducibility (2 s.d.) of standard measurements or internal precision (2 s.e.) of the data within single measurements, whichever is larger (Supplementary Table 1). n.d., not determined. [a]For single grains that were analysed multiple times, we averaged the data and calculated the corresponding uncertainties by propagating individual errors.

Mass-balance calculations[24,25] and the O isotope composition of the putative, early Solar System water[26,27] suggest that before the onset of alteration, water in the CI and other carbonaceous chondrites had a much higher $\Delta^{17}O$ value, and possibly $\delta^{18}O$ value, than the anhydrous silicates[28]. Thus, as alteration progressed, the $\Delta^{17}O$ value, and possibly the $\delta^{18}O$ value, of the altering fluid would have decreased[24,25]. The $\Delta^{17}O$ values of the carbonates and fluid will be identical at equilibrium, and thus, the $\Delta^{17}O$ values of the carbonates are a measure of the degree of progress of water–rock interactions. The $\Delta^{17}O$ values of the dolomite in the Ryugu and Ivuna samples are systematically lower than those of the calcite, and the Ryugu and Ivuna carbonates show resolvable $\Delta^{17}O$ variations beyond uncertainties (Fig. 2b). Therefore, the calcite with systematically higher $\Delta^{17}O$ values formed from less 'evolved' fluids and crystallized earlier than the dolomite. The fact that calcite is more prevalent in less-altered areas, as shown by primary anhydrous silicates, suggests that Ca was more easily leached than Mg during incipient aqueous alteration, allowing the formation of calcite before dolomite.

Like O isotopes, the C isotope compositions of carbonates are determined not only by their formation temperatures but also by the $\delta^{13}C$ values of dissolved CO_3^{2-}. The C isotope composition of CO_3^{2-} could have varied due to (1) Rayleigh-type isotopic fractionation as a result of the preferential escape of ^{12}C-rich gaseous species such as CH_4 (ref. 16), (2) the progressive formation of carbonates, that is, fractional crystallization, (3) the mixing of two or more C reservoirs with distinct $\delta^{13}C$ values that supplied CO_3^{2-} (ref. 19) or (4) the change in the chemical speciation of the C-bearing gaseous species, such as CO_2, CO and CH_4, due to varying O and H partial pressures. Rayleigh-type isotopic fractionation was not the primary mechanism for producing the observed $\delta^{13}C$ variation because it would have resulted in higher $\delta^{13}C$ values in the dolomite, which formed from the more-evolved fluids than the calcite, whereas the opposite is observed. The influence of fractional crystallization during carbonate formation was also minimal because the rare calcite that formed early presumably when a larger CO_3^{2-} pool was available displays a larger $\delta^{13}C$ variation than the more common dolomite, which is opposite to what one would expect in this scenario.

A previous study advocated that the observed $\delta^{13}C$ variation resulted from the mixing of C reservoirs with distinct $\delta^{13}C$ values reflecting the spatially heterogeneous distribution of different C reservoirs[19]. Possible C reservoirs include C-bearing gaseous species such as CO_2, CO and CH_4, originally accreted in ices, and organic matter, and the previous study invoked CO_2-bearing ices as a ^{13}C-rich reservoir[19]. However, the mixing timescales of gaseous species in the Ryugu/CI parent asteroids would have been short unless the permeability was extremely low. Therefore, the spatially heterogeneous distribution of C reservoirs would have not persisted for long. Furthermore, it is unclear why the calcite has commonly higher $\delta^{13}C$ values than the dolomite, and calcite with lower $\delta^{13}C$ values is generally absent.

Temporal change in oxygen fugacity and gaseous species

Instead of spatial heterogeneity, the temporal variation in the $\delta^{13}C$ values of the C reservoirs and their chemical speciation probably occurred due to a change in O partial pressure or, more precisely, O fugacity (fO_2), which is O partial pressure corrected for nonideal gas behaviour. Oxygen fugacity varied along with the production of H_2 via the oxidation of Fe in metal and silicates by H_2O and the subsequent escape of H_2 from the system, perhaps by diffusion or by making fractures in the parent body[29]. Thus, fO_2 was determined by the relative rates of the production and escape of H_2; in this scenario, fO_2 would have at first decreased and then increased. In the case of CM chondrites, the amount of Fe^{3+} in their matrices increases with increasing alteration[30], which is in line with this scenario.

The Fe and Mn abundances of terrestrial carbonates that reflect the Fe^{2+} and Mn^{2+} activities in fluids have been used to infer the redox conditions under which they precipitated[31]. However, the Fe and Mn abundances of Ryugu and Ivuna carbonates were probably controlled not only by redox conditions but also by the amounts of these cations leached from primary minerals during the progressive aqueous alteration[32]. Therefore, the zoning of Fe and Mn observed in the dolomite grains may not be a direct proxy for the temporal change in fO_2. Instead, here we propose that the $\delta^{13}C$ values of Ryugu and Ivuna carbonates represent a record of such temporal fO_2 variation.

To see how the $\delta^{13}C$ values of carbonates will change with varying fO_2, we consider a rather simple model, where gaseous CO_2 and CO and carbonates (and dissolved CO_2, HCO_3^- and CO_3^{2-}) are in C isotopic equilibrium, and the CO_2/CO ratio increases, corresponding to an increase in fO_2. In cometary ices, CO_2 and CO are the most abundant C-bearing chemical species[33], and the Ryugu/CI parent bodies would

https://doi.org/10.1038/s41561-023-01226-y

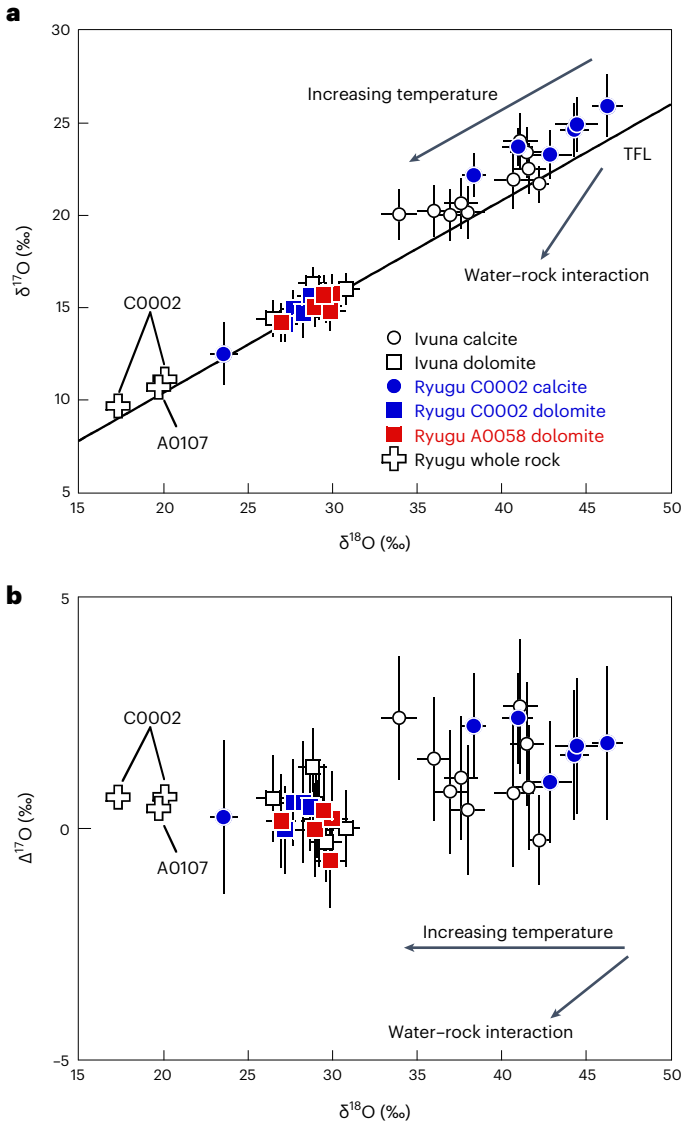

Fig. 2 | Oxygen isotope compositions of the calcite and dolomite in Ryugu and Ivuna samples. The whole-rock O isotope compositions of the Ryugu A0107 and C0002 samples[8] are also shown for reference. The changes in O isotope compositions due to variable formation temperatures and water–rock interaction are illustrated by arrows. **a**, Oxygen three-isotope plot showing $\delta^{18}O$ versus $\delta^{17}O$ values. **b**, $\delta^{18}O$ versus $\Delta^{17}O$ values. Data are presented as mean values ± 2σ errors, which are either external reproducibility (2 s.d., N = 6–20 depending on the measurement sessions) of standard measurements or internal precision (2 s.e.) of the data within single measurements, whichever is larger. TFL, terrestrial fractionation line, defined as $\delta^{17}O = 0.52 \times \delta^{18}O$.

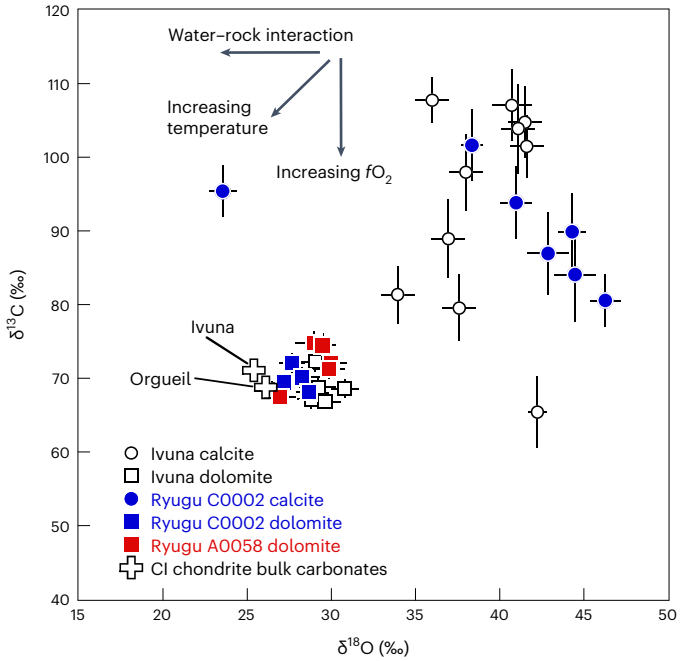

Fig. 3 | Comparison between C and O isotope compositions of the calcite and dolomite in Ryugu and Ivuna samples. The values of carbonates measured for whole-rock CI chondrites (Ivuna and Orgueil)[18] are also shown for reference. The changes in C and O isotope compositions due to variable formation temperatures and O fugacity, and water–rock interaction, are illustrated by arrows. The calcite shows much larger variations in both C and O isotope compositions than the dolomite. Note that no simple correlation between $\delta^{13}C$ and $\delta^{18}O$ values can be seen. Data are presented as mean values ± 2σ errors, which are either external reproducibility (2 s.d., N = 6–20 depending on the measurement sessions) of standard measurements or internal precision (2 s.e.) of the data within single measurements, whichever is larger.

have accreted substantial amounts of CO_2- and CO-bearing ices if they formed in the distal Solar System[11,28]. At the earliest stage of aqueous alteration, the CO_2/CO ratio may have been characterized by that of the accreted ices, which may be around unity or higher as observed for cometary ices[33,34]. We assume that the $\delta^{13}C$ value of the bulk gas (CO_2 + CO), $\delta^{13}C_{bulk}$, is constant regardless of the CO_2/CO ratio. Then the $\delta^{13}C_{bulk}$ is given by mass balance as $\delta^{13}C_{bulk} = x\delta^{13}C_{CO2} + (1-x)\,\delta^{13}C_{CO}$, where x is the mole fraction of CO_2 defined by $x = CO_2/(CO_2 + CO)$ and $\delta^{13}C_{CO2}$ and $\delta^{13}C_{CO}$ are the $\delta^{13}C$ values of CO_2 and CO, respectively. Thus, using Δ defined by $\delta^{13}C_{CO2} - \delta^{13}C_{CO}$, $\delta^{13}C_{CO2}$ and $\delta^{13}C_{CO}$ are given by $\delta^{13}C_{CO2} = \delta^{13}C_{bulk} + (1-x)\,\Delta$ and $\delta^{13}C_{CO} = \delta^{13}C_{bulk} - x\,\Delta$, respectively. The Δ value is approximated by 1,000 lnα, where α is the C isotopic fractionation factor between CO_2 and CO defined by $(^{13}C/^{12}C)_{CO2}/(^{13}C/^{12}C)_{CO}$ and is positive at all temperatures (+93‰, +76‰ and +48‰ at 0, 40 and 150 °C, respectively[21,35]). Therefore, with increasing x (and fO_2), the $\delta^{13}C$ values of both CO_2 and CO will decrease monotonically, and the $\delta^{13}C$ values of carbonates will also decrease. Thus, in this simple model, a $\delta^{13}C$ variation of carbonates comparable to the observation (~40‰) is expected if the x value varies from 0.5 to 1 (Fig. 3). The redox states evolved within a few million years after the birth of the Solar System as inferred from the ^{53}Mn–^{53}Cr chronometry of Ryugu/CI dolomite[8,10,20,36]. The presence of CH_4, another possible reducing gas, does not change this conclusion because the behaviour of CH_4 in terms of C isotopic fractionation against CO_2 is quite similar to that of CO (ref. 21). Our model where CO_2 and CO are in C isotopic equilibrium at low temperatures requires the presence of as yet unidentified processes/catalysts. The isotopic equilibrium in thermally matured natural gases has been recently discussed[37].

The characteristic $\delta^{13}C$ values of Ryugu and Ivuna carbonates are not observed for other aqueously altered meteorites such as CM chondrites and the ungrouped carbonaceous chondrite Tagish Lake[19,38,39], suggesting that the redox conditions as well as the thermal history and accreted materials are unique to their parent bodies. For example, the $\delta^{13}C$ values of CM calcite are variable like Ryugu/CI calcite, but the highest reported value (~+80‰) in CM calcite is lower than that of Ryugu/CI calcite (+108‰) (Extended Data Fig. 2). Furthermore, the $\delta^{13}C$ values of CM dolomite are also variable from ~+40‰ to ~+60‰, which is in contrast to the homogeneous $\delta^{13}C$ values observed for Ryugu/CI dolomite. Iron in CI chondrites is dominated by octahedral Fe^{3+} and indicates more-oxidized conditions than CM chondrites[30], which is consistent with the homogeneous $\delta^{13}C$ values of Ryugu/CI dolomite.

Because the $\delta^{13}C$ values of the Ryugu/CI dolomite are commonly lower and more homogeneous than those of the calcite, the dolomite probably formed at higher fO_2 and/or temperature than the calcite. This, combined with the O isotope signatures of the carbonates, implies that the calcite formed during prograde alteration over wide ranges of fO_2 and temperature, whereas the dolomite formed later during retrograde cooling when the aqueous fluids and silicates approached O isotopic equilibrium. Therefore, when the dolomite formed, the fO_2 was probably high enough that the major gaseous C reservoir was CO_2 (that is, $x \sim 1$). If correct, the $\delta^{13}C$ value of CO_2 in C isotopic equilibrium with the dolomite, which has the average $\delta^{13}C$ value of ~+70‰, would equal the $\delta^{13}C$ value of the bulk gas. Using the C isotopic fractionation factor between dolomite and CO_2, $(^{13}C/^{12}C)_{dolomite}/(^{13}C/^{12}C)_{CO2}$, of ~1.0092 at 40 °C or ~0.9951 at 150 °C (refs. 40,41), the $\delta^{13}C_{bulk}$ ($=\delta^{13}C_{CO2}$) value is estimated to be between +61‰ and +75‰.

The preceding simple model implies a $\delta^{13}C$ value higher than +60‰ for C-bearing molecules originally accreted in ices. Such ^{13}C-rich compositions are not common among Solar System materials other than meteoritic carbonates and water-soluble organic compounds[42]. A similar level of ^{13}C-enrichment ($\delta^{13}C = +65 \pm 51$‰), albeit with large uncertainty, has been reported for CO_2 in the coma of 67P/Churyumov–Gerasimenko[43]. The mechanism to produce ^{13}C-rich compositions is not well understood, but self-shielding during CO photodissociation in the solar nebula or the parent molecular cloud of the Solar System is a possible mechanism[44–46]. Thus, the inferred ^{13}C-rich composition of C-bearing molecular ices would have resulted from such physicochemical reactions[47,48], and we concluded that the Ryugu/CI parent bodies accreted materials that originated from these cold environments.

Online content

Any methods, additional references, Nature Portfolio reporting summaries, source data, extended data, supplementary information, acknowledgements, peer review information; details of author contributions and competing interests; and statements of data and code availability are available at https://doi.org/10.1038/s41561-023-01226-y.

References

1. Tachibana, S. et al. Hayabusa2: scientific importance of samples returned from C-type near-Earth asteroid (162173) 1999 JU_3. *Geochem. J.* **48**, 571–587 (2014).
2. Tachibana, S. et al. Pebbles and sand on asteroid (162173) Ryugu: in situ observation and particles returned to Earth. *Science* **375**, 1011–1016 (2022).
3. Binzel, R. P., Harris, A. W., Bus, S. J. & Burbine, T. H. Spectral properties of near-Earth objects: Palomar and IRTF results for 48 objects including spacecraft targets (9969) Braille and (10302) 1989 ML. *Icarus* **151**, 139–149 (2001).
4. Campins, H. et al. Spitzer observations of spacecraft target 162173 (1999 JU3). *Astron. Astrophys.* **503**, L17–L20 (2009).
5. Watanabe, S. et al. Hayabusa2 arrives at the carbonaceous asteroid 162173 Ryugu—a spinning top-shaped rubble pile. *Science* **364**, 268–272 (2019).
6. Sugita, S. et al. The geomorphology, color, and thermal properties of Ryugu: implications for parent-body processes. *Science* **364**, eaaw0422 (2019).
7. Kitazato, K. et al. The surface composition of asteroid 162173 Ryugu from Hayabusa2 near-infrared spectroscopy. *Science* **364**, 272–275 (2019).
8. Yokoyama, T. et al. Samples returned from the asteroid Ryugu are similar to Ivuna-type carbonaceous meteorites. *Science* **379**, eabn7850 (2023).
9. Nakamura, T. et al. Formation and evolution of carbonaceous asteroid Ryugu: direct evidence from returned samples. *Science* **379**, eabn8671 (2023).
10. Nakamura, E. et al. On the origin and evolution of the asteroid Ryugu: a comprehensive geochemical perspective. *Proc. Jpn Acad. Ser. B* **98**, 227–282 (2022).
11. Hopp, T. et al. Ryugu's nucleosynthetic heritage from the outskirts of the Solar System. *Sci. Adv.* **8**, eadd8141 (2022).
12. Paquet, M. et al. Contribution of Ryugu-like material to Earth's volatile inventory by Cu and Zn isotopic analysis. *Nat. Astron.* **7**, 182–189 (2023).
13. Moynier, F. et al. The Solar System calcium isotopic composition inferred from Ryugu samples. *Geochem. Persp. Lett.* **24**, 1–6 (2022).
14. Johnson, C. A. & Prinz, M. Carbonate compositions in CM and CI chondrites, and implications for aqueous alteration. *Geochim. Cosmochim. Acta* **57**, 2843–2852 (1993).
15. Riciputi, L. R., McSween, H. Y. Jr., Johnson, C. A. & Prinz, M. Minor and trace element concentrations in carbonates of carbonaceous chondrites, and implications for the compositions of coexisting fluids. *Geochim. Cosmochim. Acta* **58**, 1343–1351 (1994).
16. Guo, W. & Eiler, J. M. Temperatures of aqueous alteration and evidence for methane generation on the parent bodies of the CM chondrites. *Geochim. Cosmochim. Acta* **71**, 5565–5575 (2007).
17. Verdier-Paoletti, M. J. et al. Oxygen isotope constraints on the alteration temperatures of CM chondrites. *Earth Planet. Sci. Lett.* **458**, 273–281 (2017).
18. Alexander, C. M. O. 'D., Bowden, R., Fogel, M. L. & Howard, K. T. Carbonate abundances and isotopic compositions in chondrites. *Meteorit. Planet. Sci.* **50**, 810–833 (2015).
19. Fujiya, W. et al. Migration of D-type asteroids from the outer Solar System inferred from carbonate in meteorites. *Nat. Astron.* **3**, 910–915 (2019).
20. McCain, K. A. et al. Early fluid activity on Ryugu inferred by isotopic analyses of carbonates and magnetite. *Nat. Astron.* **7**, 309–317 (2023).
21. Chacko, T., Cole, D. R. & Horita, J. in *Stable Isotope Geochemistry* (eds Valley, J. W. and Cole, D. R.) 1–81 (Mineralogical Society of America, 2001).
22. Zolensky, M. E., Bourcier, W. L. & Gooding, J. L. Aqueous alteration on the hydrous asteroids: results of EQ3/6 computer simulations. *Icarus* **78**, 411–425 (1989).
23. Zheng, Y.-F. On the theoretical calculations of oxygen isotope fractionation factors for carbonate–water systems. *Geochem. J.* **45**, 341–354 (2011).
24. Clayton, R. N. & Mayeda, T. K. The oxygen isotope record in Murchison and other carbonaceous chondrites. *Earth Planet. Sci. Lett.* **67**, 151–161 (1984).
25. Marrocchi, Y., Bekaert, D. V. & Piani, L. Origin and abundance of water in carbonaceous asteroids. *Earth Planet. Sci. Lett.* **482**, 23–32 (2018).
26. Sakamoto, N. et al. Remnants of the early Solar System water enriched in heavy oxygen isotopes. *Science* **317**, 231–233 (2007).
27. Vacher, L. G., Marrocchi, Y., Verdier-Paoletti, M. J., Villeneuve, J. & Gounelle, M. Inward radial mixing of interstellar water ices in the solar protoplanetary disk. *Astrophys. J. Lett.* **827**, L1 (2016).
28. Kawasaki, N. et al. Oxygen isotopes of anhydrous primary minerals show kinship between steroid Ryugu and comet 81P/Wild2. *Sci. Adv.* **8**, eade2067 (2022).
29. Wilson, L., Keil, K., Browning, L. B., Krot, A. N. & Bourcier, W. Early aqueous alteration, explosive disruption, and reprocessing of asteroids. *Meteorit. Planet. Sci.* **34**, 541–557 (1999).
30. Beck, P. et al. The redox state of iron in the matrix of CI, CM and metamorphosed CM chondrites by XANES spectroscopy. *Geochim. Cosmochim. Acta* **99**, 305–316 (2012).

31. Barnaby, R. J. & Rimstidt, J. D. Redox conditions of calcite cementation interpreted from Mn and Fe contents of authigenic calcites. *Geol. Soc. Am. Bull.* **101**, 795–804 (1989).
32. Fujiya, W., Aoki, Y., Ushikubo, T., Hashizume, K. & Yamaguchi, A. Carbon isotopic evolution of aqueous fluids in CM chondrites: clues from *in-situ* isotope analyses within calcite grains in Yamato-791198. *Geochim. Cosmochim. Acta* **274**, 246–260 (2020).
33. Mumma, M. J. & Charnley, S. B. The chemical composition of comets—emerging taxonomies and natal heritage. *Annu. Rev. Astron. Astrophys.* **49**, 471–524 (2011).
34. Ootsubo, T. et al. AKARI near-infrared spectroscopic survey for CO_2 in 18 comets. *Astrophys. J.* **752**, 15 (2012).
35. Richet, P., Bottinga, Y. & Javoy, M. A review of hydrogen, carbon, nitrogen, and chlorine stable isotope fractionation among gaseous molecules. *Annu. Rev. Earth Planet. Sci.* **5**, 65–110 (1977).
36. Fujiya, W., Sugiura, N., Sano, Y. & Hiyagon, H. Mn–Cr ages of dolomites in CI chondrites and the Tagish Lake ungrouped carbonaceous chondrite. *Earth Planet. Sci. Lett.* **362**, 130–142 (2013).
37. Thiagarajan, N. et al. Isotopic evidence for quasi-equilibrium chemistry in thermally mature natural gases. *Proc. Natl Acad. Sci. USA* **117**, 3989–3995 (2017).
38. Telus, M., Alexander, C. M. O. 'D., Hauri, E. H. & Wang, J. Calcite and dolomite formation in the CM parent body: insight from *in situ* C and O isotope analyses. *Geochim. Cosmochim. Acta* **260**, 275–291 (2019).
39. Vacher, L. G., Marrocchi, Y., Villeneuve, J., Verdier-Paoletti, M. J. & Gounelle, M. Petrographic and C & O isotopic characteristics of the earliest stages of aqueous alteration of CM chondrites. *Geochim. Cosmochim. Acta* **213**, 271–290 (2017).
40. Sheppard, S. M. F. & Schwarcz, H. P. Fractionation of carbon and oxygen isotopes and magnesium between coexisting metamorphic calcite and dolomite. *Contrib. Mineral. Petrol.* **26**, 161–198 (1970).
41. Romanek, C. S., Grossman, E. L. & Morse, J. W. Carbon isotopic fractionation in synthetic aragonite and calcite: effects of temperature and precipitation rate. *Geochim. Cosmochim. Acta* **56**, 419–430 (1992).
42. Aponte, J. C., McLain, H. L., Dworkin, J. P. & Elsila, J. E. Aliphatic amines in Antarctic CR2, CM2, and CM1/2 carbonaceous chondrites. *Geochim. Cosmochim. Acta* **189**, 296–311 (2016).
43. Hässig, M. et al. Isotopic composition of CO_2 in the coma of 67P/Churyumov-Gerasimenko measured with ROSINA/DFMS. *Astron. Astrophys.* **605**, A50 (2017).
44. Yurimoto, H. & Kuramoto, K. Molecular cloud origin for the oxygen isotope heterogeneity in the Solar System. *Science* **305**, 1763–1766 (2004).
45. Lyons, J. R. & Young, E. D. CO self-shielding as the origin of oxygen isotope anomalies in the early solar nebula. *Nature* **435**, 317–320 (2005).
46. Lyons, J. R., Gharib-Nezhad, E. & Ayres, T. R. A light carbon isotope composition for the Sun. *Nat. Commun.* **9**, 908 (2018).
47. Visser, R., van Dishoeck, E. F. & Black, J. H. The photodissociation and chemistry of CO isotopologues: applications to interstellar clouds and circumstellar disks. *Astron. Astrophys.* **503**, 323–353 (2009).
48. Woods, P. M. & Willacy, K. Carbon isotope fractionation in protoplanetary disks. *Astrophys. J.* **693**, 1360–1378 (2009).

Wataru Fujiya[1] ✉, Noriyuki Kawasaki[2], Kazuhide Nagashima[3], Naoya Sakamoto[4], Conel M. O'D. Alexander[5], Noriko T. Kita[6], Kouki Kitajima[6], Yoshinari Abe[7], Jérôme Aléon[8], Sachiko Amari[9,10], Yuri Amelin[11], Ken-ichi Bajo[2], Martin Bizzarro[12], Audrey Bouvier[13], Richard W. Carlson[5], Marc Chaussidon[14], Byeon-Gak Choi[15], Nicolas Dauphas[16], Andrew M. Davis[16], Tommaso Di Rocco[17], Ryota Fukai[18], Ikshu Gautam[19], Makiko K. Haba[19], Yuki Hibiya[20], Hiroshi Hidaka[21], Hisashi Homma[22], Peter Hoppe[23], Gary R. Huss[3], Kiyohiro Ichida[24], Tsuyoshi Iizuka[25], Trevor R. Ireland[26], Akira Ishikawa[19], Shoichi Itoh[27], Thorsten Kleine[28], Shintaro Komatani[24], Alexander N. Krot[3], Ming-Chang Liu[29,30], Yuki Masuda[19], Kevin D. McKeegan[29], Mayu Morita[24], Kazuko Motomura[31], Frédéric Moynier[14], Izumi Nakai[32], Ann Nguyen[33], Larry Nittler[5], Morihiko Onose[24], Andreas Pack[17], Changkun Park[34], Laurette Piani[35], Liping Qin[36], Sara S. Russell[37], Maria Schönbächler[38], Lauren Tafla[29], Haolan Tang[29], Kentaro Terada[39], Yasuko Terada[40], Tomohiro Usui[18], Sohei Wada[2], Meenakshi Wadhwa[41], Richard J. Walker[42], Katsuyuki Yamashita[43], Qing-Zhu Yin[44], Tetsuya Yokoyama[19], Shigekazu Yoneda[45], Edward D. Young[29], Hiroharu Yui[46], Ai-Cheng Zhang[47], Tomoki Nakamura[48], Hiroshi Naraoka[49], Takaaki Noguchi[27], Ryuji Okazaki[49], Kanako Sakamoto[18], Hikaru Yabuta[50], Masanao Abe[18], Akiko Miyazaki[18], Aiko Nakato[18], Masahiro Nishimura[18], Tatsuaki Okada[18], Toru Yada[18], Kasumi Yogata[18], Satoru Nakazawa[18], Takanao Saiki[18], Satoshi Tanaka[18], Fuyuto Terui[51], Yuichi Tsuda[18], Sei-ichiro Watanabe[21], Makoto Yoshikawa[18], Shogo Tachibana[52] & Hisayoshi Yurimoto[2]

[1]Faculty of Science, Ibaraki University, Mito, Japan. [2]Department of Natural History Sciences, Hokkaido University, Sapporo, Japan. [3]Hawai'i Institute of Geophysics and Planetology, University of Hawai'i at Mānoa, Honolulu, HI, USA. [4]Isotope Imaging Laboratory, Creative Research Institution, Hokkaido University, Sapporo, Japan. [5]Earth and Planets Laboratory, Carnegie Institution for Science, Washington, DC, USA. [6]Geoscience, University of Wisconsin–Madison, Madison, WI, USA. [7]Graduate School of Engineering Materials Science and Engineering, Tokyo Denki University, Tokyo, Japan. [8]Institut de Minéralogie, de Physique des Matériaux et de Cosmochimie, Sorbonne Université, Museum National d'Histoire Naturelle, CNRS UMR 7590, IRD, Paris, France. [9]McDonnell Center for the Space Sciences and Physics Department, Washington University, St Louis, MO, USA. [10]Geochemical Research Center,

The University of Tokyo, Tokyo, Japan. [11]Guangzhou Institute of Geochemistry, Chinese Academy of Sciences, Guangzhou, China. [12]Centre for Star and Planet Formation, GLOBE Institute, University of Copenhagen, Copenhagen, Denmark. [13]Bayerisches Geoinstitut, Universität Bayreuth, Bayreuth, Germany. [14]Université Paris Cité, Institut de Physique du Globe de Paris, CNRS, Paris, France. [15]Department of Earth Science Education, Seoul National University, Seoul, Republic of Korea. [16]Department of the Geophysical Sciences and Enrico Fermi Institute, The University of Chicago, Chicago, IL, USA. [17]Faculty of Geosciences and Geography, University of Göttingen, Göttingen, Germany. [18]ISAS/JSEC, JAXA, Sagamihara, Japan. [19]Department of Earth and Planetary Sciences, Tokyo Institute of Technology, Tokyo, Japan. [20]Research Center for Advanced Science and Technology, The University of Tokyo, Tokyo, Japan. [21]Earth and Planetary Sciences, Nagoya University, Nagoya, Japan. [22]Osaka Application Laboratory, SBUWDX, Rigaku Corporation, Osaka, Japan. [23]Max Planck Institute for Chemistry, Mainz, Germany. [24]Analytical Technology, Horiba Techno Service Co., Ltd, Kyoto, Japan. [25]Earth and Planetary Science, The University of Tokyo, Tokyo, Japan. [26]School of Earth and Environmental Sciences, The University of Queensland, St Lucia, Queensland, Australia. [27]Earth and Planetary Sciences, Kyoto University, Kyoto, Japan. [28]Max Planck Institute for Solar System Research, Göttingen, Germany. [29]Earth, Planetary, and Space Sciences, UCLA, Los Angeles, CA, USA. [30]Lawrence Livermore National Laboratory, Livermore, CA, USA. [31]Thermal Analysis, Rigaku Corporation, Tokyo, Japan. [32]Applied Chemistry, Tokyo University of Science, Tokyo, Japan. [33]Astromaterials Research and Exploration Science, NASA Johnson Space Center, Houston, TX, USA. [34]Earth-System Sciences, Korea Polar Research Institute, Incheon, Korea. [35]Centre de Recherches Pétrographiques et Géochimiques, CNRS - Université de Lorraine, Nancy, France. [36]School of Earth and Space Sciences, University of Science and Technology of China, Hefei, China. [37]Department of Earth Sciences, Natural History Museum, London, UK. [38]Institute for Geochemistry and Petrology, Department of Earth Sciences, ETH Zurich, Zurich, Switzerland. [39]Earth and Space Science, Osaka University, Osaka, Japan. [40]Spectroscopy and Imaging, Japan Synchrotron Radiation Research Institute, Hyogo, Japan. [41]School of Earth and Space Exploration, Arizona State University, Tempe, AZ, USA. [42]Geology, University of Maryland, College Park, MD, USA. [43]Graduate School of Natural Science and Technology, Okayama University, Okayama, Japan. [44]Earth and Planetary Sciences, University of California, Davis, CA, USA. [45]Science and Engineering, National Museum of Nature and Science, Tsukuba, Japan. [46]Chemistry, Tokyo University of Science, Tokyo, Japan. [47]School of Earth Sciences and Engineering, Nanjing University, Nanjing, China. [48]Department of Earth Science, Tohoku University, Sendai, Japan. [49]Department of Earth and Planetary Sciences, Kyushu University, Fukuoka, Japan. [50]Earth and Planetary Systems Science Program, Hiroshima University, Higashi-Hiroshima, Japan. [51]Kanagawa Institute of Technology, Atsugi, Japan. [52]UTokyo Organization for Planetary and Space Science, University of Tokyo, Tokyo, Japan. ✉e-mail: wataru.fujiya.sci@vc.ibaraki.ac.jp

Methods

Isotope measurement using ion microprobe

We produced the polished sections of Ryugu samples A0058-C1001 and C0002-C1001 and Ivuna embedded in epoxy[8,28]. The polished sections were coated with a thin (~5 nm) gold film using a Leica EM ACE600 coater at Hokkaido University for backscattered electron and X-ray imaging as well as elemental analysis, which were conducted before in-situ O and C isotope measurements. We observed their mineralogy and petrology and located carbonate grains using a field-emission scanning electron microscope (JEOL JSM-7000F) equipped with an energy-dispersive X-ray spectrometer (Oxford X-Max 150) at Hokkaido University. The beam currents were ~2 nA and ~1 nA for the X-ray mapping and quantitative analysis, respectively. Quantitative calculations were conducted using Oxford AZtec software.

We selected five and four dolomite grains from the Ryugu samples A0058 and C0002, respectively, and nine calcite grains from C0002 for isotope analyses. We also analysed seven dolomite grains and ten calcite grains from Ivuna. Before the isotope analyses, the samples were coated again with an additional thin (~65 nm) gold film.

We conducted the O and C isotope measurements of the selected carbonate grains using secondary ion mass spectrometry (SIMS; CAMECA ims-1280HR) at Hokkaido University. Instrumental mass fractionation was corrected using the UWC3 calcite standard and a series of dolomite–ankerite standards from the WiscSIMS laboratory for calcite and dolomite, respectively[49–51]. Measurement spots were observed using the field-emission scanning electron microscope after the SIMS measurements, and data from spots with inclusions or overlapping matrix minerals were rejected. The reported uncertainties (2σ) of isotope compositions are the larger of the external reproducibility (2 s.d. of standard measurements) or internal precision (2 s.e. of data within single measurements of unknown samples) (Supplementary Table 1).

The procedures of O isotope measurement of dolomite were described by a previous study[8]. For O isotope measurement of calcite, as previously described for the O isotope measurement of olivine[28], secondary $^{16}O^-$, $^{17}O^-$ and $^{18}O^-$ ions produced by a Cs^+ primary ion beam (~30 pA, ~3 μm) were simultaneously collected using Faraday cup (10^{11} Ω), electron multiplier (EM) and EM detectors, respectively. Mass-resolving power was >6,000, sufficient to resolve $^{17}O^-$ from $^{16}OH^-$. The secondary ion intensities of $^{16}O^-$ were 2–3 × 10^7 cps. The measurement time was 240 s. The $^{16}OH^-$ count rate was measured immediately after each measurement, and we made a small tail correction on $^{17}O^-$; its contribution to $^{17}O^-$ was typically less than ~0.1‰ and up to ~0.5‰ for a few analyses. The typical uncertainties of $\delta^{17}O$, $\delta^{18}O$ and $\Delta^{17}O$ values were 1.4‰, 0.9‰ and 1.4‰, respectively.

For C isotope measurement of dolomite, secondary $^{12}C^-$ and $^{13}C^-$ ions produced by a Cs^+ primary ion (~50 pA, ~2 μm) were simultaneously collected using Faraday cup (10^{12} Ω) and EM detectors, respectively. We scanned the primary ion beam across 1 × 1-μm-sized areas to make the SIMS pits shallower and suppress ratio drifts during measurements. Mass-resolving power was ~4,500, sufficient to resolve $^{13}C^-$ from $^{12}CH^-$. The secondary ion intensities of $^{12}C^-$ were 5–6 × 10^5 cps. The measurement time was 480 s. The typical uncertainty of $\delta^{13}C$ values was 1.3‰.

For C isotope measurement of calcite, secondary $^{12}C^-$ and $^{13}C^-$ ions produced by a Cs^+ primary ion (~3 pA, ~1 μm) were simultaneously collected using two EM detectors. We scanned the primary ion beam on 1 × 1-μm-sized areas. Mass-resolving power was ~4,500. The secondary ion intensities of $^{12}C^-$ were ~2 × 10^4 cps. The measurement time was 800 s. The typical uncertainty of $\delta^{13}C$ values was 5.1‰. The larger uncertainty of the calcite measurement was due to the smaller primary ion beam intensity than for the dolomite measurement to analyse small calcite grains.

Data availability

All data generated or analysed during this study are included in this published article (and its supplementary information files) and are available via Zenodo (https://doi.org/10.5281/zenodo.7957625). As the initial analysis of Ryugu samples collected by the Hayabusa2 spacecraft, the specimens analysed in this study were allocated to us by JAXA. The Ivuna specimen used in this study was kindly proved by the Natural History Museum, UK.

References

49. Kozdon, R., Ushikubo, T., Kita, N. T., Spicuzza, M. & Valley, J. W. Intratest oxygen isotope variability in the planktonic foraminifer *N. pachyderma*: real vs. apparent vital effects by ion microprobe. *Chem. Geol.* **258**, 327–337 (2009).
50. Śliwiński, M. G. et al. Secondary ion mass spectrometry bias on isotope ratios in dolomite–ankerite, part I: $\delta^{18}O$ matrix effects. *Geostand. Geoanal. Res.* **40**, 157–172 (2015).
51. Śliwiński, M. G. et al. Secondary ion mass spectrometry bias on isotope ratios in dolomite-ankerite, part II: $\delta^{13}C$ matrix effects. *Geostand. Geoanal. Res.* **40**, 173–184 (2015).

Acknowledgements

We thank D. Rogers, M. Spicuzza and J. Valley for the preparation of carbonate standard materials for SIMS measurements and A. Tsuchiyama for discussion. Hayabusa2 was developed and built under the leadership of Japan Aerospace Exploration Agency (JAXA), with contributions from the German Aerospace Center (DLR) and the Centre National d'Études Spatiales (CNES), and in collaboration with NASA, and other universities, institutes and companies in Japan. The curation system was developed by JAXA in collaboration with companies in Japan. This research was supported in part by the JSPS KAKENHI grant numbers 19H00725 (W.F.), 20K20934 (W.F. and T.N.) and 22K18722 (N.K.).

Author contributions

W.F., N.K., K.N., N.S. and H. Yurimoto designed this study and T. Nakamura, H.N., T. Noguchi, R.O., K.S., H. Yabuta, M.A., A.M., A. Nakato, M.N., T.O., T. Yada, K. Yogata, S.N., T.S., S. Tanaka, F.T., Y. Tsuda, S. Watanabe, M.Y. and S. Tachibana supported them. W.F., N.K., K.N., N.S. and H. Yurimoto analysed the samples, and N.T.K. and K.K. assisted the analysis. W.F., N.K., K.N. and H. Yurimoto were involved in data reduction. C.M.O'D.A., Y. Abe, J.A., S.A., Y. Amelin, K.B., M.B., A.B., R.W.C., M.C., B.-G.C., N.D., A.M.D., T.D.R., R.F., I.G., M.K.H., Y.H., H. Hidaka., H. Homma, P.H., G.R.H., K.I., T.I., T.R.I., A.I., S.I., T.K., S.K., A.N.K., M.-C.L., Y.M., K.D.M., M.M., K.M., F.M., I.N., A. Nguyen, L.N., M.O., A.P., C.P., L.P., L.Q., S.S.R., M.S., L.T., H.T., K.T., Y. Terada, T.U., S. Wada, M.W., R.J.W., K. Yamashita, Q.-Z.Y., T. Yokoyama, S.Y., E.D.Y., H. Yui and A.-C.Z. contributed to data interpretation. W.F. wrote the paper with support and approval of all co-authors.

Competing interests

The authors declare no competing interests.

Additional information

Extended data is available for this paper at https://doi.org/10.1038/s41561-023-01226-y.

Supplementary information The online version contains supplementary material available at https://doi.org/10.1038/s41561-023-01226-y.

Correspondence and requests for materials should be addressed to Wataru Fujiya.

Peer review information *Nature Geoscience* thanks John Eiler, Michael Zolensky and Christopher Herd for their contribution to the peer review of this work. Primary Handling Editors: Stefan Lachowycz and Alison Hunt, in collaboration with the *Nature Geoscience* team.

https://doi.org/10.1038/s41561-023-01226-y

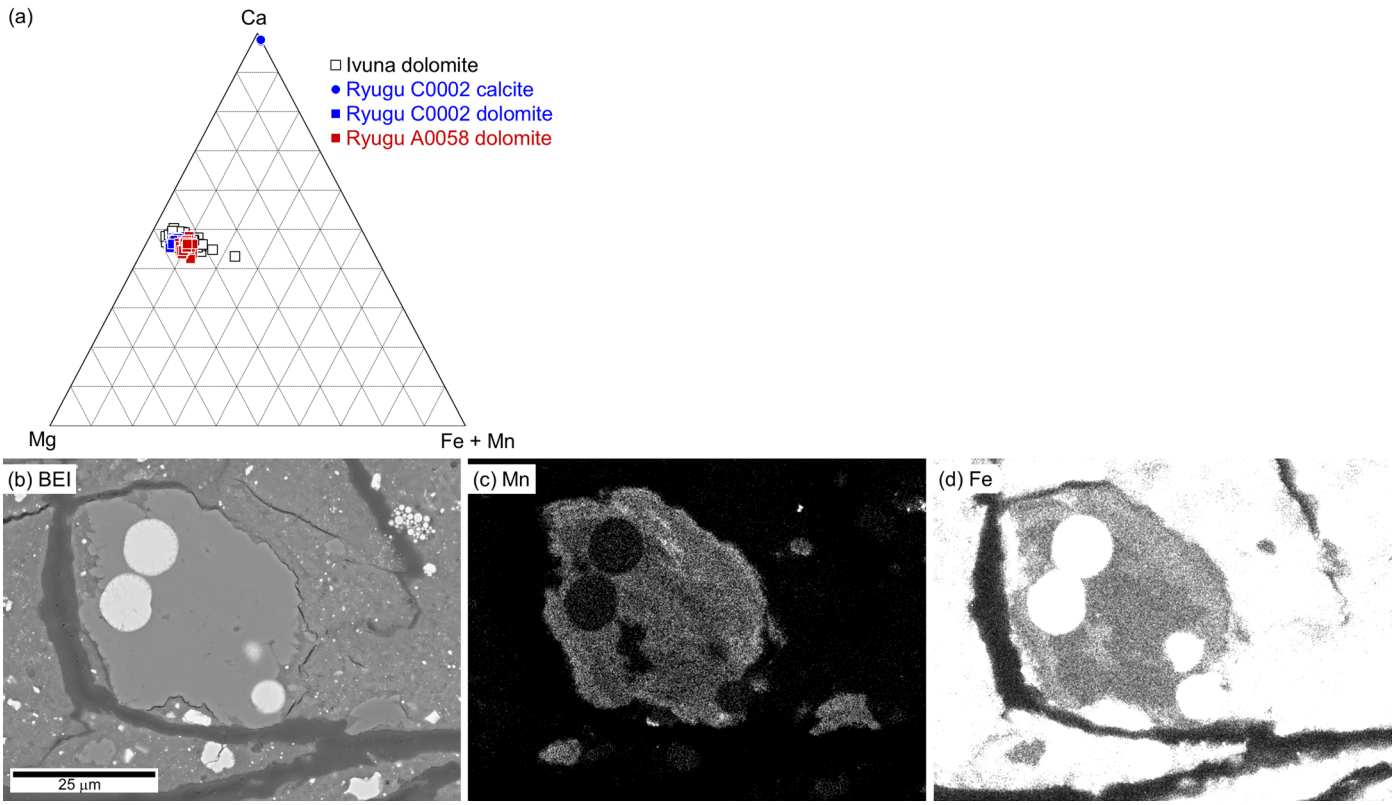

Extended Data Fig. 1 | Compositional variation of Ryugu and Ivuna carbonates. (a) Ternary diagram of dolomite and calcite in Ryugu and Ivuna samples (see also Supplementary Table 1). (b-d) Backscattered electron image: BEI **(b)**, Mn Kα_1 X-ray map (**c**), Fe Kα_1 X-ray map (**d**) of a dolomite grain in the Ryugu C0002 sample.

https://doi.org/10.1038/s41561-023-01226-y

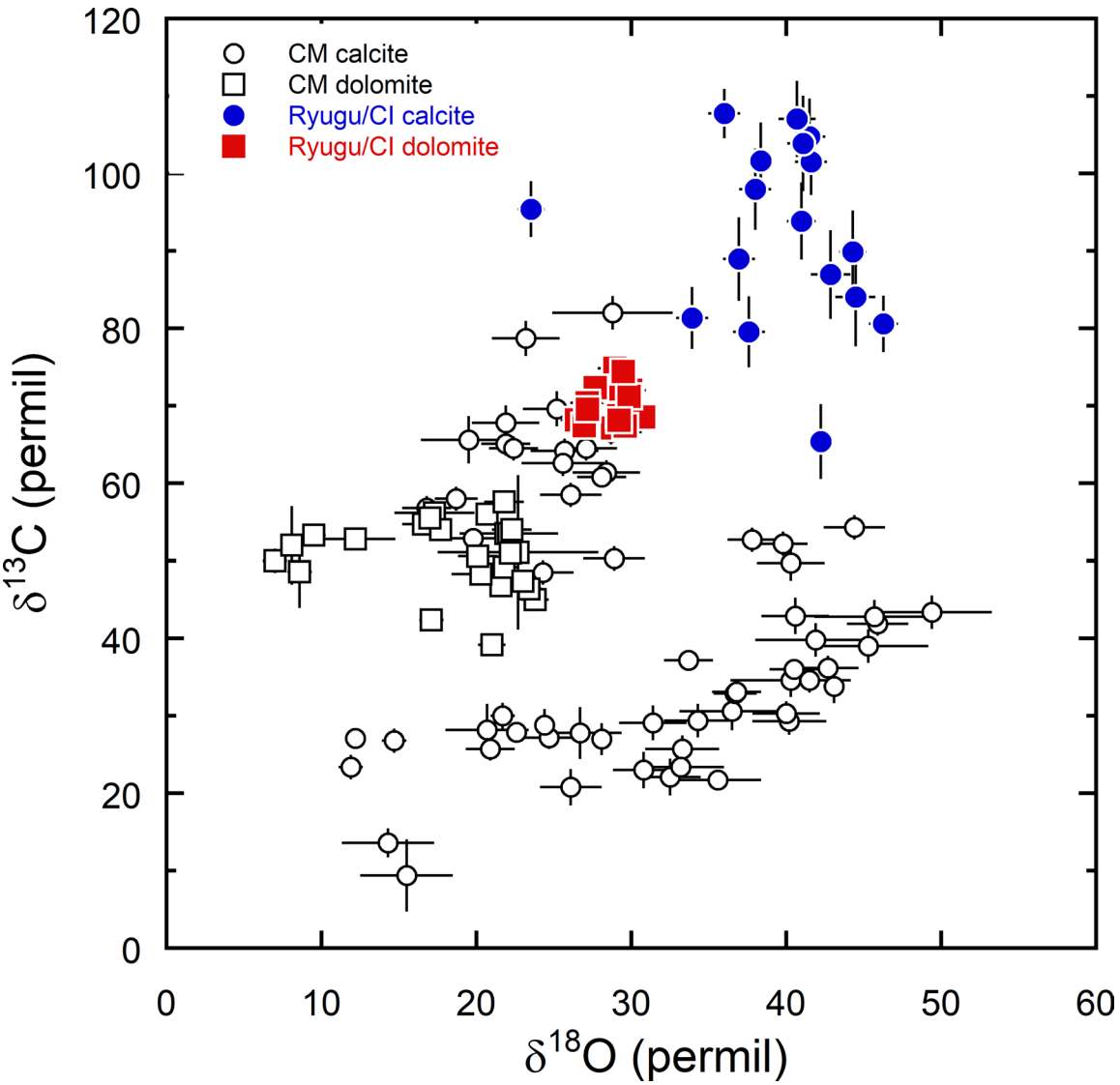

Extended Data Fig. 2 | Comparison between C and O isotope compositions of carbonates in Ryugu, CI, and CM chondrites. CM chondrite data are taken from Telus et al. (ref. 38). The $\delta^{13}C$ values of CM calcite are variable like Ryugu/CI calcite, but the highest reported value in CM calcite is lower than that of Ryugu/CI calcite. The $\delta^{13}C$ and $\delta^{18}O$ values of CM dolomite are also variable, whereas those of Ryugu/CI dolomite are more homogeneous. Data generated during this study are presented as mean values ± 2σ errors which are either external reproducibility (2 SD, $N = 6–20$ depending on the measurement sessions) of standard measurements or internal precision (2SE) of the data within single measurements, whichever is larger.